Regular Article

PHYSICAL CHEMISTRY RESEARCH
Published by the
Iranian Chemical Society
www.physchemres.org
info@physchemres.org

***Phys. Chem. Res.**, Vol. 5, No. 2, 317-328, June 2017*
DOI: 10.22036/pcr.2016.56926.1274

Application of GMA Equation of State to Study Thermodynamic Properties of 2-Amino-2-methyl-1-propanol as an Efficient Absorbent for CO_2

S. Naderi, E.K. Goharshadi* and H. Ahmadzadeh
Department of Chemistry, Ferdowsi University of Mashhad, Mashhad 9177948974, Iran
(Received 29 June 2016, Accepted 21 December 2016)

Alkanolamine solutions such as 2-amino-2-methyl-1-propanol (AMP) are widely used in chemical industries for the removal of acid gases such as CO_2 and H_2S. In this work, the density of CO_2, AMP, water, and AMP solutions using the Goharshadi-Morsali-Abbaspour Equation of State "GMA EoS" in the extended 50-degree range of temperatures (313.06-362.65 K) and pressures (0.5-40 MPa) was calculated. The results showed that the GMA EoS can reproduce the density of these fluids within experimental errors throughout the liquid phase. The minimum and maximum absolute average deviations for the prediction of density for all studied fluids are -0.0082 and 5.2288, respectively. The values of statistical parameters between experimental and calculated thermodynamic properties such as isobaric expansion coefficient, isothermal compressibility, internal pressure, and solubility parameter of AMP show the ability of this equation of state in reproducing these properties.

Keywords: Alkanolamine, CO_2 removal, Equation of state, Solubility parameter

INTRODUCTION

Climate change is one of the most alarming global environmental concerns. It is mainly caused by increasing atmospheric carbon dioxide originating from industrial activities [1]. The most common sources of CO_2 pollution are mobile sources such as transportation and electricity generation power stations that burn fossil fuels. There is an international collaboration to lower the level of CO_2 in the atmosphere but this level is approaching 400 parts per million in 2015. This level has not been seen on earth in millions of years. Because of the clear and present danger of CO_2 level, 195 countries summoned in Paris last December and reached an agreement to significantly lower their carbon emissions during the next 30 years [2]. CO_2 removal is accomplished by three main strategies: (1) chemical reaction-based techniques (2) direct injection underground, and (3) bioremediation [3]. Chemical reaction is the most promising and widely used technology for CO_2 removal [4].

*Corresponding author. E-mail: gohari@um.ac.ir

Amine-based absorbents such as alkanolamines including monoethanolamine [5], 2-amino-2-methyl-1-propanol (AMP) [6], triethanolamine [7], carbonate systems [8] and amino acid salts [9] have been used for CO_2 capture from flue gases.

Accurate prediction of the thermodynamic properties of CO_2 absorbents is of fundamental importance in the design, optimization, and operation of absorption based CO_2 capture processes. The equation of state (EoS) is a major tool for calculating the thermodynamic properties of fluids [10].

The aim of the present work is to report the results of the calculations of thermodynamic properties for CO_2, AMP, and AMP solutions using the Goharshadi-Morsali-Abbaspour Equation of State "GMA EoS" [11]. AMP is a sterically hindered primary amine with relatively fast reaction kinetics, low regeneration energy, and a greater CO_2 loading capacity than other primary amines [9].

The parameters of an empirical equation like Tait correlations are fitted to the experimental data of some specified fluids and hence they have no physical meaning. Also, they are accurate only for the target fluids within the

range of experimental data for which their parameters are fitted, however they may be unreliable outside the range or for other fluids. In contrast, the GMA EoS is based on the average potential energy and tested for a wide variety of fluids including polar, nonpolar, and hydrogen-bonded fluids [10-14]. The GMA EoS is based on the average potential energy and is given as [11]:

$$(2Z-1)V_m^3 = A(T,X) + B(T,X)\rho \tag{1}$$

where Z, V_m and ρ are compressibility factor, molar volume, and density of the fluid, respectively. The intercept and slope of this equation depend on temperature *via* the equations:

$$A(T,X) = A_o - \frac{2A_1}{RT} + \frac{2A_2 \ln T}{R} \tag{2}$$

$$B(T,X) = B_o - \frac{2B_1}{RT} + \frac{2B_2 \ln T}{R} \tag{3}$$

where A_o, A_1, A_2 and B_o, B_1, and B_2 are constants. To use the equation of state for a liquid, A and B parameters must be known. To find these parameters, we may plot $(2Z\text{-}1)V^3_m$ against ρ for different isotherms. The slope and intercept of the straight lines can be fitted with Eqs. (2) and (3) from which *As* and *Bs* can be found. The GMA EoS is valid for $T < T_C$ and $\rho > \rho_C$.

The composition dependence of the parameters of GMA EoS are given by the following equations:

$$A = \sum_i^n \sum_j^n x_i x_j A_{ij} \tag{4}$$

$$B = \sum_i^n \sum_j^n x_i x_j B_{ij} \tag{5}$$

The values of A_{ij} and B_{ij} when $i = j$ can be obtained from experimental *P-V-T* data of pure fluids. The parameters of A_{ij} and B_{ij}, for $i \neq j$, have been calculated using one binary mixture. For example, for a binary mixture we can write

$$A = x_1^2 A_{11} + 2x_1 x_2 A_{12} + x_2^2 A_{22} \tag{6}$$

$$B = x_1^2 B_{11} + 2x_1 x_2 B_{12} + x_2^2 B_{22} \tag{7}$$

One way to compute the parameters of A_{ij} and B_{ij} is to use a "combining rule". The most common such rule is the mean geometric rule. That is:

$$A_{ij} = \sqrt{A_{ii} A_{jj}} \tag{8}$$

$$B_{ij} = \sqrt{B_{ii} B_{jj}} \tag{9}$$

RESULTS AND DISCUSSION

Experimental Test of GMA EoS

We used the experimental *PVT* data of liquid water [15], liquid AMP [16], CO_2 [17] and different mixtures of AMP + water [16] at various temperatures to examine the linearity of $(2Z\text{-}1)V_m^3$ *vs.* ρ (Eq. (1)) and the results are shown in Fig. 1. In fact, using the experimental *PVT* data, we calculated $(2Z\text{-}1)V_m^3$ for each liquid at any temperature and pressure. Fig. 1 and Tables 1 and 2 show that the linearity (Eq. (1)) holds very well for each fluid. Table 1 gives the intercept, *A,* and slope, *B,* of the fitted straight line of Eq. (1), and the square of correlation coefficient, R^2, for liquid water, liquid AMP, and different mixtures of AMP + water at different temperatures and compositions. Both the slope and the intercept depend on the temperature as well as the composition of the mixture. In general, as the mole fraction of AMP increases, the absolute values of *A* and *B* increase whereas by raising the temperature, these values decrease. This reflects the change of strength of the intermolecular interactions with composition and temperature. Table 2 gives the values of *A* and *B* for CO_2 along with R^2 values confirming CO_2 obeys the GMA EoS.

Table 3 gives the values of constants of Eqs. (2) and (3) and correlation coefficients for water, AMP, AMP + water solutions. Table 4 gives these values for CO_2. These constants are necessary to calculate the thermodynamic properties of these fluids like density at each temperature or mole fraction as discussed in the next section.

Thermodynamic Properties

The density of all fluids was calculated as a second check of the GMA EoS by the following equation using the

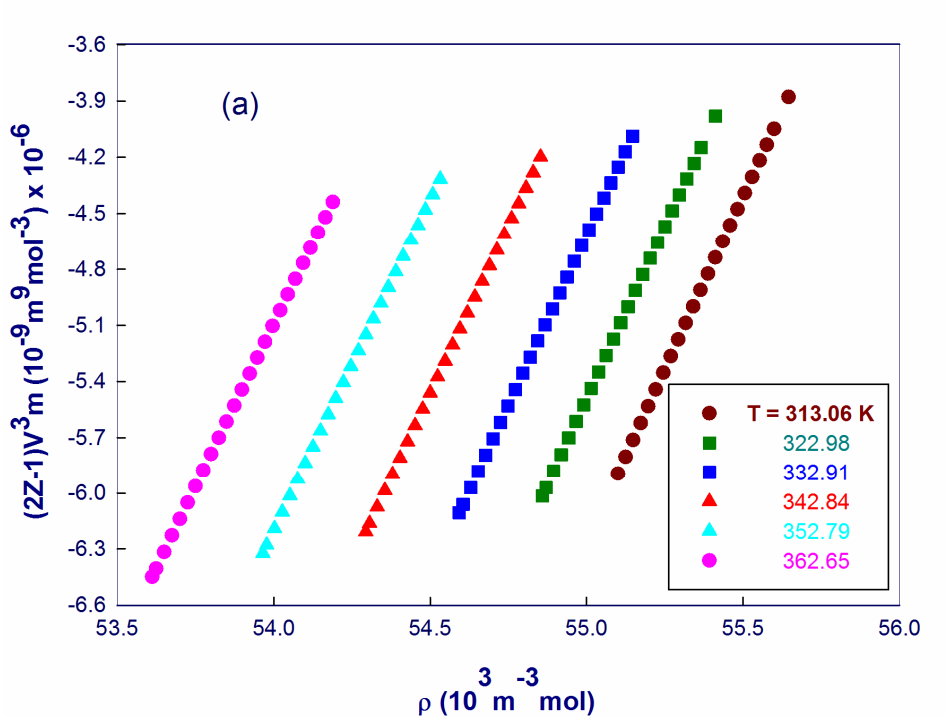
(a)
T = 313.06 K
322.98
332.91
342.84
352.79
362.65
(2Z-1)V³m (10⁻⁹m⁹mol⁻³) x 10⁻⁶
ρ (10³ m⁻³ mol)

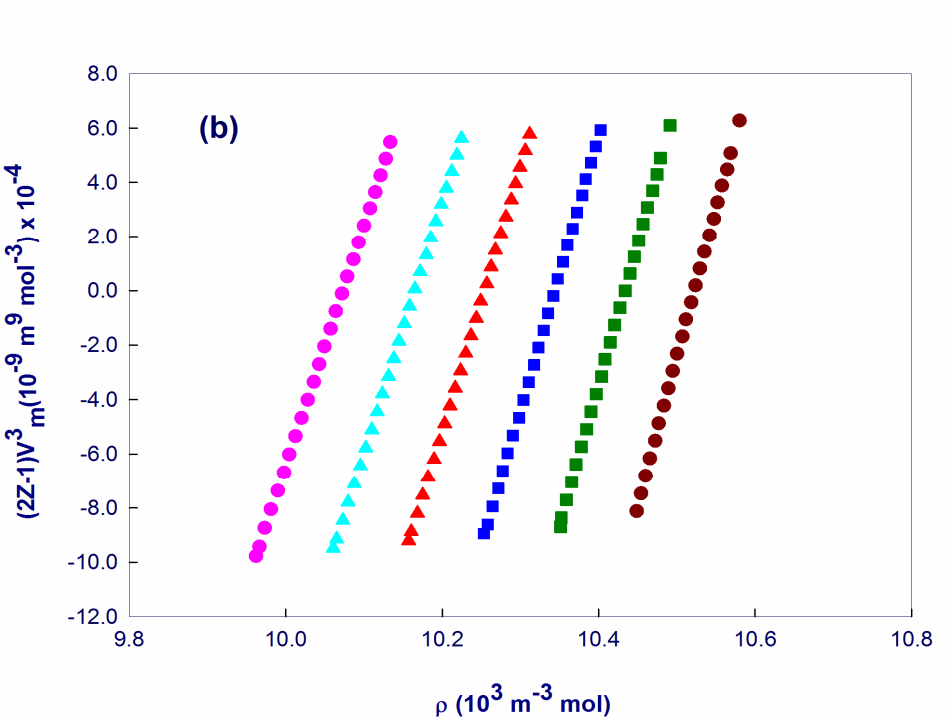
(b)
(2Z-1)V³m(10⁻⁹ m⁹ mol⁻³) x 10⁻⁴
ρ (10³ m⁻³ mol)

Fig. 1.

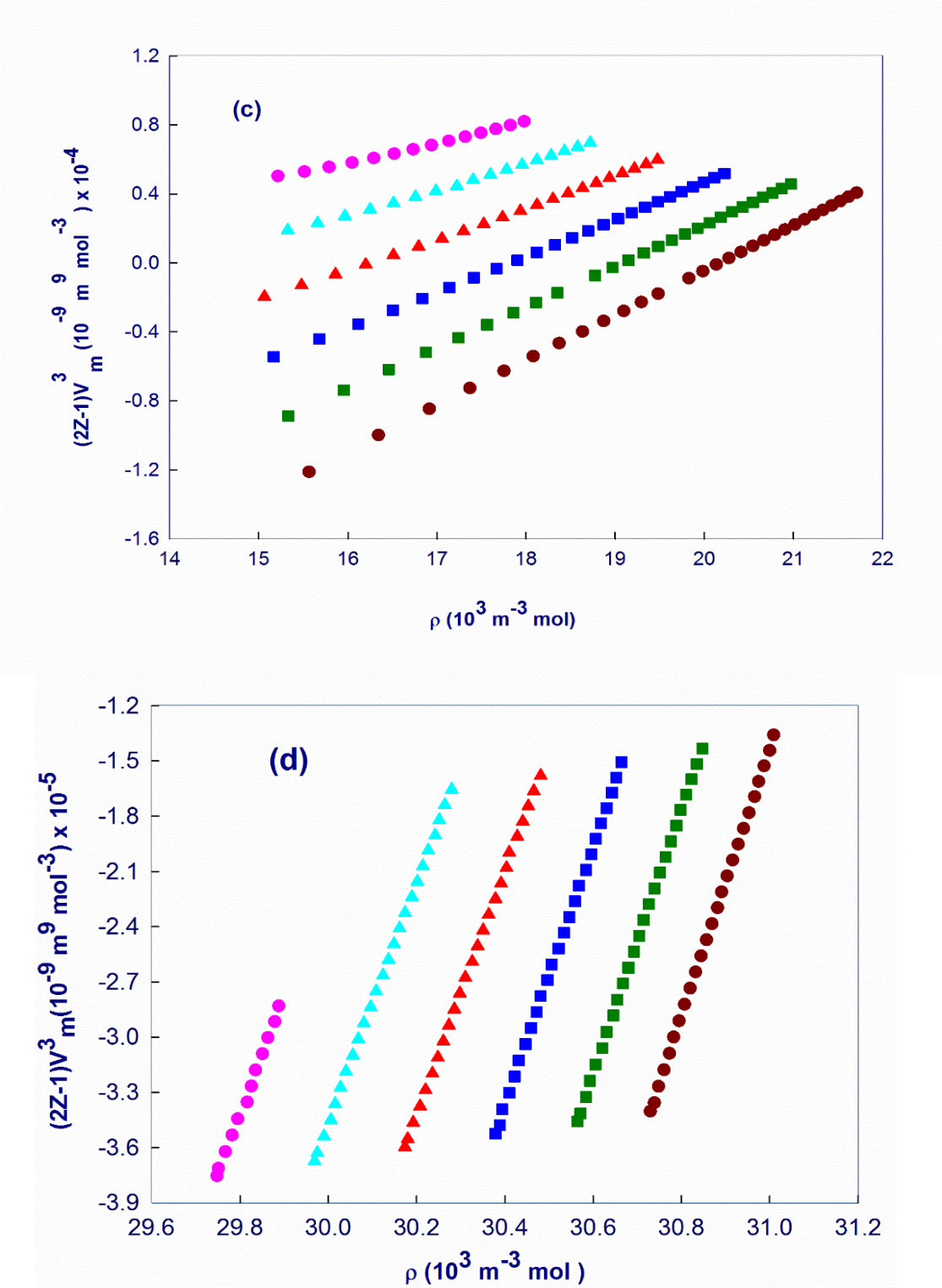

Fig. 1. Isotherms of $(2Z-1)V^3_m$ *vs.* ρ for (a) Liquid water (b) Liquid AMP (c) CO_2 (d) AMP (x = 0.1997) + water solution.

Table 1. The Intercept, Slope and Square of Correlation Coefficient of Eq. (1) for AMP (x) + Water (1-x)

x	T (K)	$-A(T) \times 10^{-4}$ (10^{-9} m^9 mol^{-3})	$B(T) \times 10^{-6}$ (10^{-12} m^{12} mol^{-4})	R^2	x	T (K)	$-A(T) \times 10^{-4}$ (10^{-9} m^9 mol^{-3})	$B(T) \times 10^{-6}$ (10^{-12} m^{12} mol^{-4})	R^2
0.0000	313.06	2.095	3.696	0.9999	0.4002	313.13	98.54	459.9	0.9997
	322.98	2.078	3.678	0.9999		323.10	94.97	446.3	0.9997
	332.91	2.049	3.642	0.9999		333.05	90.62	428.9	0.9999
	342.84	2.015	3.597	0.9999		342.93	86.06	410.3	0.9998
	352.79	1.976	3.544	0.9999		352.87	83.25	399.9	0.9998
	362.65	1.933	3.486	0.9999		362.74	79.69	385.8	0.9999
0.1997	313.13	22.69	72.73	0.9998	0.4976	313.13	165.2	893.1	0.9998
	323.10	22.30	71.82	0.9998		323.09	160.0	871.9	0.9998
	332.99	21.66	70.14	0.9997		333.04	154.1	846.1	0.9998
	342.92	20.32	66.16	0.9997		342.92	144.7	800.8	0.9998
	352.86	19.88	65.12	0.9997		352.87	140.4	783.2	0.9999
	362.74	19.52	64.37	0.9971		362.73	133.3	750.3	0.9999
0.2821	313.13	45.11	171.5	0.9998	1.0000	313.06	1147	10900	0.9997
	323.08	43.79	167.4	0.9998		322.98	1090	10450	0.9998
	332.01	42.06	161.7	0.9998		332.91	1040	10050	0.9998
	342.91	39.59	153.2	0.9998		342.84	991.6	9672	0.9998
	352.85	38.57	150.2	0.9998		352.79	939.8	924.6	0.9999
	362.73	37.00	145.1	0.9998		362.65	890.3	883.8	0.9999

GMA EoS constants given in Tables 3 and 4:

$$B(T,x)\rho^5 + A(T,x)\rho^4 + \rho - \frac{2P}{RT} = 0 \tag{10}$$

The calculated densities were compared with their corresponding experimental data using the statistical parameters, namely, the absolute average deviation (AAD) and the average percentage deviation (bias):

$$AAD = \frac{1}{N}\sum_{i=1}^{N} 100\left|\frac{Y_{\exp} - Y_{cal}}{Y_{\exp}}\right| \tag{11}$$

$$bias = \frac{1}{N}\sum_{i=1}^{N} 100\left(\frac{Y_{\exp} - Y_{cal}}{Y_{\exp}}\right) \tag{12}$$

where Y stands for a thermodynamic property. As Table 5 shows the values of AAD and bias confirm that the GMA EoS can reproduce the density of water, AMP, AMP + water solutions, and CO_2 very well within the experimental errors.

The isobaric expansion coefficient, α, isothermal compressibility, β, internal pressure, P_i, for AMP and AMP + water solutions were calculated using GMA EoS. The functions used for calculating these properties using GMA

Table 2. The Intercept, Slope and Square of Correlation Coefficient of Eq. (1) for CO_2

T (K)	$-A(T) \times 10^{-4}$ (10^{-9} m^9 mol^{-3})	$B(T) \times 10^{-5}$ (10^{-12} m^{12} mol^{-4})	R^2
313.06	-5.2730	2.6150	0.9999
322.98	-4.5310	2.3760	0.9999
332.91	-3.7560	2.1100	0.9997
342.84	-2.9460	1.8140	0.9991
352.79	-2.3250	1.6120	0.9990
362.65	-1.2750	1.1590	0.9953

Table 3. Values of Constants for Eqs. (2) and (3) for AMP (x) + Water (1-x)

x	A_0 (10^{-9} m^9 mol^{-3})	A_1 (10^{-7}m^{12} Pa mol^{-4})	A_2 (10^{-7} m^{12} Pa mol^{-4} K^{-1}) $\times 10^5$	R^2	B_o (10^{-12} m^{12} mol^{-4})	B_1 (10^{-10} m^{15} Pa mol^{-5})	B_2 (10^{-10} m^{15} Pa mol^{-5} K^{-1}) $\times 10^{-6}$	R^2
0.0000	-1.3980	-0.5851	883.90	0.9969	0.15150	0.1221	-936.5000	0.9979
0.1997	-0.0037	0.0247	2.411	0.9639	0.00010	-0.0006	-0.7057	0.9482
0.2821	-0.0081	0.0591	5.807	0.9981	0.00270	0.0029	-16.1980	0.9976
0.4002	-0.0189	0.1333	10.410	0.9972	0.00080	-0.0052	-5.5325	0.9960
0.4976	-0.4068	-0.5331	250. 00	0.9929	0.02200	0.0311	-100.0000	0.9893
1.0000	-0.0065	-0.0113	3.8271	0.9997	0.00009	0.0002	0.5795	0.9993

Table 4. Values of Constants for Eqs. (2) and (3) for CO_2

A_0 (10^{-9} m^9 mol^{-3})	A_1 (10^{-7} m^{12} Pa mol^{-4})	A_2 (10^{-7} m^{12} Pa mol^{-4} K^{-1}) $\times 10^5$	R^2	B_o (10^{-12} m^{12} mol^{-4})	B_1 (10^{-10} m^{15} Pa mol^{-5})	B_2 (10^{-10} m^{15} Pa mol^{-5} K^{-1}) $\times 10^{-6}$	R^2
-0.05907	-0.08761	1.2620-4	0.9971	3.4590e-3	5.8390e-3	-7.3090e-6	0.9932

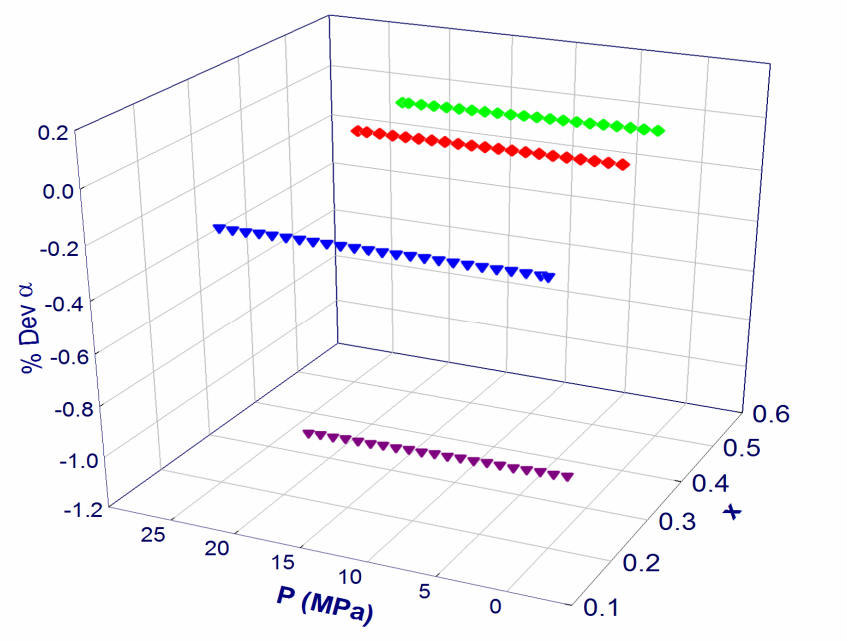

Fig. 2. Three-dimensional deviation plot between calculated and experimental [15] isobaric thermal expansion coefficients for AMP (x) + water mixture (1-x) for different compositions at 313.13 K. The symbols are the same as Fig. 1.

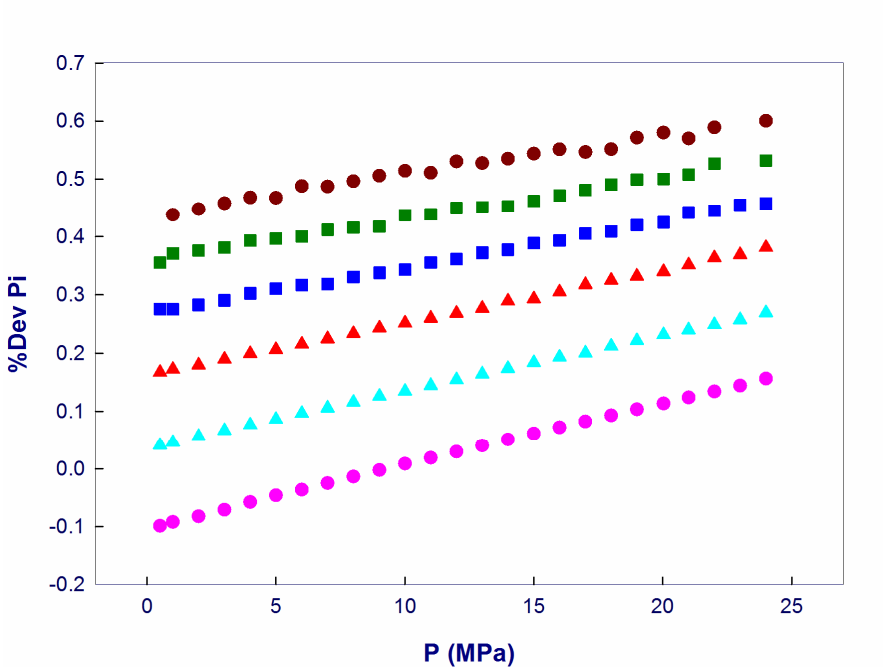

Fig. 3. The deviation plot of calculated and experimental [16] internal pressure versus pressure for AMP at different temperatures. The symbols are the same as Fig. 1.

Table 5. AAD and Bias of Calculated and Experimental Density Values for Water [15], AMP [16], and CO_2 [17], and AMP (x) + Water (1-x) [16] at Different Temperatures

Compound	T (K)	AAD	Bias
H_2O	313.06	0.0530	-0.0530
	322.98	0.0451	0.0451
	332.91	0.0342	0.0192
	342.84	0.0264	0.0264
	352.79	0.0275	0.0275
	362.65	0.0436	0.0436
0.1997 AMP+0.8003 H_2O	313.13	0.1045	-0.1045
	323.10	0.0110	-0.0110
	332.99	0.0205	0.0205
	342.92	0.0165	0.0165
	352.86	0.0082	-0.0077
	362.74	0.0827	-0.0827
0.2821 AMP+0.7179 H_2O	313.13	0.5502	-0.5502
	323.08	0.0805	-0.0805
	332.01	0.0730	0.0730
	342.91	0.1599	0.1599
	352.85	0.0242	-0.0242
	362.73	0.4561	-0.4561
0.4002 AMP+0.5998 H_2O	313.13	0.0149	0.0149
	323.10	0.0312	0.0312
	333.05	0.0406	0.0406
	342.93	0.0285	0.0285
	352.87	0.0374	0.8747
	362.74	0.0278	0.0278
0.4967 AMP+0.5033 H_2O	313.13	0.2286	-0.2286
	323.09	0.2370	-0.2370
	333.04	0.2487	-0.2487
	342.92	0.2723	-0.2723
	352.87	0.2574	-0.2574
	362.73	0.2382	-0.2382
AMP	313.06	0.4562	-0.4562
	322.98	0.3720	0.1637
	332.91	0.3616	0.1143
	342.84	0.4145	0.1469
	352.79	0.4482	0.1531
	362.65	0.4671	0.1373
CO_2	332.91	5.2288	2.7732
	342.84	3.6550	-0.0417
	352.79	0.9370	0.0086
	362.65	2.8949	-2.8942

Table 6. AAD and Bias of the Calculated and Experimental [16] Isobaric Thermal Expansion Coefficients and Isothermal Compressibility Coefficients for AMP

T (K)	AAD	Bias
Isobaric thermal expansion coefficient		
313.06	4.1438	4.2375
322.98	3.6823	-0.7007
332.92	3.1758	3.1758
342.84	3.4738	-0.7809
352.79	4.2042	-1.9004
362.65	4.9299	-3.7697
Isothermal compressibility coefficient		
313.06	1.7613	1.1873
322.98	5.2350	-3.6867
332.92	6.1470	-5.0364
342.84	5.5232	-3.7464
352.79	5.8700	-4.4174
362.65	6.5020	-5.6749

EoS are given as follows:

$$\alpha = \frac{\left(2B_1 + 2B_2T\right)\rho^5 + \left(2A_1 + 2A_2T\right)\rho^4 + 2P}{5\rho^5\left(RT^2B_o - 2B_1T + 2T^2B_2\ln T\right) + 4\rho^4\left(A_oRT^2 - 2A_1T + 2A_2T^2\ln T\right) + RT^2\rho} \quad (13)$$

$$\beta = \frac{2}{\rho RT + 4\rho^4\left(RTA_o - 2A_1 + 2TA_2\ln T\right) + 5\rho^5\left(B_oRT - 2B_1 + 2B_2T\ln T\right)} \quad (14)$$

$$P_i = \left(B_1 + B_2T\right)\rho^5 + \left(A_1 + A_2T\right)\rho^4 \quad (15)$$

To calculate thermodynamic properties of each compound at any temperature and pressure, we used the values of A_o, A_1, A_2 and B_o, B_1, and B_2 given in Table 3 and inserted in the above corresponding equations. Figure 2 shows the three-dimensional deviation plot between the calculated and experimental isobaric thermal expansion coefficient for the AMP + water solutions for different compositions at 313.13 K. As this figure shows there is a good agreement between the experimental isobaric thermal expansion coefficient and corresponding calculated coefficients based on GMA EoS.

The isobaric thermal expansion coefficient and isothermal compressibility coefficient for AMP were calculated and compared with their corresponding experimental data using the statistical parameters of AAD and bias and the results are given in Table 6. As this table shows GMA EoS can reproduce the experimental data for the isobaric thermal expansion coefficient and isothermal compressibility coefficient of AMP with a good accuracy. Figure 3 shows the deviation between calculated and

Table 7. The Experimental and Calculated Values of Solubility Parameter of AMP at Different Temperatures and Pressures

T (K)	*P* (M Pa)	δ (M $Pa^{1/2}$) Cal.	Exp. [16]	Dev. (%)
313.06	1.0000	21.5182	21.5654	0.2188
	6.0000	21.4858	21.5384	0.2442
	12.0000	21.4448	21.5019	0.2655
	18.0020	21.4014	21.4607	0.2763
	24.0040	21.3558	21.4201	0.3002
322.98	1.0000	21.6018	21.6420	0.1857
	6.0000	21.5756	21.6189	0.2003
	12.0000	21.5416	21.5902	0.2251
	18.0020	21.5051	21.5581	0.2458
	24.0040	21.4662	21.5235	0.2662
332.91	1.0000	21.6659	21.6939	0.1290
	6.0000	21.6441	21.6785	0.1587
	12.0010	21.6173	21.6564	0.1805
	18.0020	21.5878	21.6321	0.2048
	24.0040	21.5555	21.6050	0.2291
342.84	1.0000	21.7076	21.7251	0.0805
	6.0000	21.6928	21.7162	0.1077
	12.0000	21.6735	21.7026	0.1340
	18.0020	21.6510	21.6863	0.1628
	24.0040	21.6256	21.6701	0.2053
352.79	1.0000	21.7296	21.7346	0.0230
	6.0000	21.7228	21.7333	0.0483
	12.0000	21.7113	21.7280	0.0768
	18.0020	21.6962	21.7193	0.1063
	24.0040	21.6779	21.7071	0.1345
362.65	1.0020	21.7340	21.7240	-0.0460
	6.0000	21.7344	21.7305	-0.0180
	12.0000	21.7311	21.7343	0.0147
	18.0020	21.7238	21.7339	0.0465
	24.0030	21.7128	21.7298	0.0782

experimental internal pressure at different temperatures while pressures for AMP is very low. Hence, GMA EoS can reproduce the internal pressure of AMP within the experimental errors.

The Hildebrand solubility parameter provides an extensive and qualitative sign of the mutual solubility behavior for most solvent/solute systems [18]. Hildebrand [19] proposed the square root of cohesive energy density as a numerical value for the solubility parameter of a specific solvent. Table 7 gives the experimental [16] and calculated values of solubility parameter of AMP at different temperatures and pressures. Our results show that the solubility parameter of AMP decreases with increasing the pressure at constant temperature. As pressure increases the

cohesive forces become weak and hence the solubility parameter of a liquid decreases. The solubility parameter of AMP increases with increasing temperature at constant pressure whereas the solubility of most liquids decreases with increasing temperature at constant pressure. The solubility parameter is based on the regular solution model. It may be alkanolamines like liquid metals [20] that are totally different from regular solutions and hence their properties are not the same.

CONCLUSIONS

The present work has the following main conclusions:

1. EoS model was used to calculate different thermodynamic properties of AMP and AMP solutions using analytical expressions as functions of both temperature and pressure.
2. GMA EoS is applicable to complex cases of systems forming hydrogen bonding such as alkanolamines.
3. The proposed model provides a simple, reliable, and fast method to predict different thermodynamic properties of AMP.

ACKNOWLEDGEMENTS

The authors acknowledge Ferdowsi University of Mashhad for supporting this project (3/ 37962).

REFERENCES

[1] Aronu, U. E.; Hessen, E. T.; Haug-Warberg, T.; Hoff, K. A.; Svendsen, H. F., Equilibrium absorption of carbon dioxide by amino acid salt and amine amino acid salt solutions. *Energy procedia,* **2011**, *4*, 109-116. DOI: 10.1016/j.egypro.2011.01.030

[2] ICAP. 2016, Emissions Trading Worldwide: Status Report 2016. Berlin: ICAP.

[3] Raeesossadati, M.; Ahmadzadeh, H.; McHenry, M.; Moheimani, N., CO_2 bioremediation by microalgae in photobioreactors: Impacts of biomass and CO_2 concentrations, light, and temperature. *Algal Res.,* **2014**, 6, 78-85.DOI: 10.1016/j.algal.2014.09.007.

[4] Mondal, M. K.; Balsora, H. K.; Varshney, P., Progress and trends in CO_2 capture/separation technologies: a review. *Energy,* **2012**, *46*, 431-441. DOI: 10.1016/ j.energy.2012.08.006.

[5] Mertens, J.; Lepaumier, H.; Desagher, D.; Thielens, M. -L., Understanding ethanolamine (MEA) and ammonia emissions from amine based post combustion carbon capture: Lessons learned from field tests. *Int. J. Greenhouse Gas Control,* **2013**, *13*, 72-77. DOI: 10.1016/j.ijggc.2012.12.013.

[6] Kim, Y. E.; Lim, J. A.; Jeong, S. K.; Yoon, Y. I.; Bae, S. T.; Nam, S. C., Comparison of carbon dioxide absorption in aqueous MEA, DEA, TEA and AMP solutions. *Bull. Korean Chem. Soc.,* **2013**, *34*, 783-787. DOI: 10.5012/bkcs.2013.34.3.783.

[7] Knuutila, H.; Juliussen, O.; Svendsen, H. F., Kinetics of the reaction of carbon dioxide with aqueous sodium and potassium carbonate solutions. *Chem. Eng. Sci.,* **2010**, *65*, 6077-6088. DOI: 10.1016/ j.ces.2010.07.018.

[8] Aronu, U. E.; Hartono, A.; Svendsen, H. F., Kinetics of carbon dioxide absorption into aqueous amine amino acid salt: 3-(methylamino) propylamine/ sarcosine solution. *Chem. Eng. Sci.,* **2011**, *66*, 6109-6119. DOI: 10.1016/j.ces.2011.08.036.

[9] Song, H. -J.; Park, S.; Kim, H.; Gaur, A.; Park, J. -W.; Lee, S. -J., Carbon dioxide absorption characteristics of aqueous amino acid salt solutions. *Int. J. Greenhouse Gas Control,* **2012**, *11*, 64-72. DOI: 10.1016/j.ijggc.2012.07.019.

[10] Goharshadi, E.; Moosavi, M., Extension of a new equation of state to the liquid mixtures. *Ind. Eng. Chem. Res.,* **2005**, *44*, 6973-6980. DOI: 10.1021/ ie050158y.

[11] Goharshadi, E. K.; Morsali, A.; Abbaspour, M., New regularities and an equation of state for liquids. *Fluid Phase Equilib.,* **2005**, *230*, 170-175. DOI: 10.1016/ j.fluid.2004.12.010.

[12] Goharshadi, E. K.; Moosavi, M., Thermodynamic properties of some ionic liquids using a simple equation of state. *J. Mol. Liq.,* **2008**, *142*, 41-44. DOI: 10.1016/j.molliq.2008.04.005.

[13] Goharshadi, E. K.; Imani, M.; Rahimi-Zarei, R.; Razghandi, F.; Abareshi, M.; Berenji, A. R., Prediction of excess thermodynamic functions and activity coefficients of some polymeric liquid

mixtures using a new equation of state. *Eur. Polym. J.,* **2010**, *46*, 587-591. DOI: 10.1016/j.eurpolymj.2009.11.008.

[14] Goharshadi, E. K.; Azizi-Toupkanloo, H., Validity of some regularities of dense fluids for ionic liquids. *J. Mol. Liq.,* **2010**, *151*, 117-121. DOI: 10.1016/j.molliq.2009.12.001

[15] www.peacesoftware.de/einigewerte/wasser_dampf_e.html.

[16] Zúñiga-Moreno, A.; Galicia-Luna, L. A.; Bernal-García, J. M.; Iglesias-Silva, G. A., Densities and derived thermodynamic properties of 2-amino-2-methyl-1-propanol + water mixtures at temperatures from (313-363) K and pressures up to 24 MPa. *J. Chem. Eng. Data,* **2008**, *53*, 100-107. DOI: 10.1021/je700406p.

[17] www.carbon-dioxide-properties.com.

[18] Williams, L. L.; Rubin, J. B.; Edwards, H., Calculation of hansen solubility parameter values for a range of pressure and temperature conditions, including the supercritical fluid region. *Ind. Eng. Chem. Res.,* **2004**, *43*, 4967-4972. DOI: 10.1021/ie0497543.

[19] J. Hildebrand, The solubility of non-electrolytes, Reinhold, New York, 1936.

[20] Goharshadi, E. K.; Hesabi, M., Estimation of solubility parameter using equations of state. *J. Mol. Liq.,* **2004**, *113*, 125-132. DOI: 10.1016/j.molliq.2004.02.030.